Huge isotope effect on the vibrational lifetimes of an $H_2^*(C)$ defect in Si

T. M. Gibbons and S. K. Estreicher*
Physics Department, Texas Tech University, Lubbock, Texas 79409-1051, USA

K. Potter, F. Bekisli, and M. Stavola
Physics Department, Lehigh University, Bethlehem, Pennsylvania 18015, USA

(Received 25 December 2012; published 13 March 2013)

The hydrogenation of C-rich Si leads to the formation of two (almost) energetically degenerate $H_2^*(C)$ complexes, each containing one substitutional C (C_s) and two interstitial H atoms which are located at a bond-centered (bc) and an antibonding (ab) site, respectively. The two defects are trigonal: C_s-$H_{bc}\cdots$Si-H_{ab} and H_{ab}-$C_s\cdots H_{bc}$-Si. Fourier-transform infrared (FTIR) absorption spectra of these two defects should show two C_s-H and two Si-H stretch modes, but the H_{ab}-C_s mode was absent in earlier studies. The missing line has now been observed by FTIR in especially C rich Si material. The line is unexpectedly broad, suggesting a very short vibrational lifetime. Partial D substitutions result in the formation of a H_{ab}-$C_s\cdots D_{bc}$-Si center. In this defect, the H_{ab}-C_s line shifts by only 0.3 cm^{-1} but becomes very sharp, suggesting a long lifetime. The IR line widths show that the vibrational lifetime of the H_{ab}-C_s mode in H_{ab}-$C_s\cdots D_{bc}$-Si is about 16 times longer than that of the same H_{ab}-C_s mode in H_{ab}-$C_s\cdots H_{bc}$-Si. This paper contains experimental data and first-principles calculations which explain this isotope effect.

DOI: 10.1103/PhysRevB.87.115207 PACS number(s): 63.20.kg, 63.20.dd, 63.20.dk

I. INTRODUCTION

Multi- and monocrystalline cast Si are commonly used to fabricate solar cells. These cells are hydrogenated in order to passivate bulk defects. The hydrogenation is achieved by the postdeposition anneal of a H-rich SiN_x antireflection coating[1] and H concentrations of the order of 10^{15} cm^{-3} are achieved[2,3] throughout the bulk of the sample. About one order of magnitude higher concentrations of H are obtained by annealing the sample near the melting point in an H_2 ambient followed by rapid quenching.[4] Cast Si material is C rich. The intensity of the Fourier-transform infrared (FTIR) absorption line of substitutional carbon (C_s) shows that its concentration[5] can reach 10^{18} cm^{-3}, above the solubility limit of C in Si.[6] This is presumably due to the fast cooling rate of cast Si relative to monocrystalline materials and the high C concentration in the source material and furnace environment.

Hydrogenation of C-rich Si results in the formation of H-related defects that are different from those observed in floating-zone or Czochralski-grown Si. Indeed, in low-C material, most of the H introduced forms interstitial H_2 molecules.[7–9] In C-rich Si, FTIR studies show that two $H_2^*(C)$ (also called CH_2^*), C_2H_2, and VH_4 complexes dominate at low temperatures.[5] Each of the two trigonal and (almost) energetically degenerate $H_2^*(C)$ defects contains one C_s and two H atoms which are located at a bond-centered (bc) and an antibonding (ab) site, respectively: C_s-$H_{bc}\cdots$Si-H_{ab} and H_{ab}-$C_s\cdots H_{bc}$-Si. These two defects are the reservoir from which H is released at ∼300 °C. The C_2H_2 defect is also trigonal. It consists of two adjacent C_s's with two H atoms facing each other at bc sites: C_s-$H_{bc}\cdots H_{bc}$-C_s.[10] This configuration is stable up to ∼900 °C.[5] Finally, VH_4 is the fully saturated vacancy. It becomes mobile at ∼550 °C, traps at C_s, and forms a VH_3CH center from which H is released at ∼650 °C.[11,12]

The existence of a pair of $H_2^*(C)$ defects was predicted by theory.[13] These calculations, performed in small H-saturated clusters, show that the two configurations have energies within 0.02 eV of each other, are electrically inactive, and should exhibit IR-active stretch modes at 3004 and 2135 cm^{-1} (in the case of C_s-$H_{bc}\cdots$Si-H_{ab}) and 3053 and 2412 cm^{-1} (in the case of H_{ab}-$C_s\cdots H_{bc}$-Si). The higher frequency corresponds to the C-H stretch mode in each case. FTIR studies[14] resulted in the observation of the local vibrational modes (LVMs) associated with the C_s-$H_{bc}\cdots$Si-H_{ab} defect, with LVMs at 2752 (C_s-H_{bc} stretch), 1921.8 (Si-H_{ab} stretch), and 792.0 (Si-H_{ab} wag) cm^{-1}.

Joint experimental (FTIR with uniaxial stress and D substitutions) and theoretical (density-functional studies in Si_{64} periodic supercells) studies[15] identified the two $H_2^*(C)$ defects, and the theoretical results were later confirmed.[16] The C_s-$H_{bc}\cdots$Si-H_{ab} and H_{ab}-$C_s\cdots H_{bc}$-Si structures are trigonal, almost energetically degenerate (within less than 0.1 eV), stable up to ∼300 °C, electrically inactive, and characterized by three stretch modes and one wag mode. At low temperatures, they are (in cm^{-1}) 2752.3 (C_s-H_{bc} stretch), 1921.8 (Si-H_{ab} stretch), 792 (Si-H_{ab} wag), and 2210.4 (H_{bc}-Si stretch). While it is not uncommon for wag modes to be broad and therefore difficult to see in FTIR spectra, the high-frequency H_{ab}-C_s stretch mode should be visible. Yet, it was not observed.

The missing H_{ab}-C_s stretch mode has been detected by FTIR in C-rich samples.[5] The line is broad, suggesting that its vibrational lifetime (τ) is short. D substitutions lead to the formation of the H_{ab}-$C_s\cdots D_{bc}$-Si center. Its H_{ab}-C_s line shifts by 0.3 cm^{-1} and becomes very narrow, suggesting a much longer τ.

Direct measurements of vibrational lifetimes[17] involve transient bleaching spectroscopy and access to a fast-pulse laser. However, τ can also be estimated from the IR line width. Indeed, the lifetime of a LVM is inversely proportional to the IR line width at low temperatures, in the low defect concentration limit. Since other sources of line broadening are possible, the measured line width only provides a lower limit on τ. In the Si host, the τ's determined by transient bleaching

and by low-temperature IR measurements have been consistent for those cases where both strategies could be used.[18]

The number of phonons involved in the decay can be estimated from the lifetime via the empirical "frequency-gap law."[19] Two-phonon decays correspond to τ's of the order of 4 to 10 ps, three-phonon decays range from 30 to 90 ps, etc.

The experimental data relevant to the IR line width of H_{ab}-C_s in the H_{ab}-$C_s \cdots H_{bc}$-Si and its D/H isotope substitutions are described in Sec. II. The calculations of the vibrational lifetimes and decay channels are described in Sec. III. The key results are discussed in Sec. IV.

II. OBSERVATION OF THE H_{ab}-C_s STRETCH MODE

A. Experimental procedure

Multicrystalline Si samples containing a high C concentration (8×10^{17} cm^{-3}) were used for our FTIR studies. The Si grains are large, ranging from a few millimeters to 1 cm in size. Samples were cut with typical dimensions $6 \times 8 \times 15$ mm^3 and viewed with the probing IR light propagating along the long axis of the sample. Hydrogen (or mixtures of H and D) were introduced into our Si samples by annealing in an H_2 (or $H_2 + D_2$) ambient at 1250 °C in sealed quartz ampoules followed by a rapid quench to room temperature.

IR spectra were measured with a Bomem DA3 Fourier transform IR spectrometer. An InSb detector (77 K) was used for measurements of H stretching modes. The highest resolution available with our spectrometer is 0.026 cm^{-1}, a value that was verified by measurements of the rovibrational lines of gas phase CO_2 and H_2O present in the spectrometer ambient. Samples were cooled to near 4.2 K with a Helitran, continuous-flow cryostat. Temperature was measured with a Chromel-Au: 0.07 at. % Fe thermocouple placed a few millimeters from the sample.

B. Measured frequencies and line widths

We have measured vibrational spectra for the H stretching lines of the H_2^*(C) defect assigned previously to the trigonal H_{ab}-$C_s \cdots H_{bc}$-Si structure with sufficiently high resolutions to determine the widths of the IR lines at low temperature. The lines were fitted with Lorentzian line shapes to determine their widths. The frequencies and line widths determined by our measurements are listed in Table I. The H_{bc}-Si mode has a line width of 0.11 cm^{-1}. However, the H_{ab}-C_s line at 2688.3 cm^{-1} has a width of 2.2 cm^{-1}, a value that is sufficiently large to have impeded the observation of this H stretching mode in early studies. The full width at half maximum (FWHM) of the IR line, Γ_H, measured at low temperature provides a lower limit for the lifetime of the vibrational mode, given by $\Gamma_H = (2\pi c\tau)^{-1}$. The lifetimes that correspond to the measured line widths are also listed in Table I.

TABLE I. Frequencies (cm^{-1}), FWHM (cm^{-1}), and vibrational lifetimes τ (ps) at 4.2 K of the H stretch modes for the H_{ab}-$C_s \cdots H_{bc}$-Si center in Si and its partially deuterated isotopic siblings.

Defect	Bond	Frequency	FWHM	τ
H_{ab}-$C_s \cdots H_{bc}$-Si	H_{ab}-C_s	2688.3	2.2	2.4
H_{ab}-$C_s \cdots H_{bc}$-Si	H_{bc}-Si	2210.4	0.11	47
D_{ab}-$C_s \cdots H_{bc}$-Si	H_{bc}-Si	2214.7	0.18	29
H_{ab}-$C_s \cdots D_{bc}$-Si	H_{ab}-C_s	2688.6	0.14	39

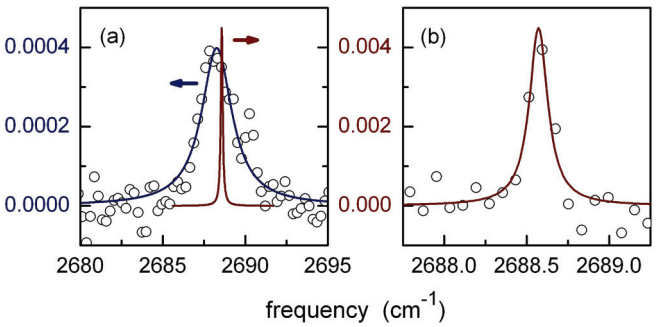

FIG. 1. (Color online) (a) Absorbance of the IR spectra (4.2 K) for the H_{ab}-C_s mode. The broad line (H_{ab}-$C_s \cdots H_{bc}$-Si) was measured with a resolution of 0.5 cm^{-1}. The narrower line (H_{ab}-$C_s \cdots D_{bc}$-Si) was measured with a resolution of 0.05 cm^{-1}. The solid lines show fits of Lorentzian line shapes to the IR data. (b) Expansion of the horizontal scale for the H_{ab}-C_s mode of the H_{ab}-$C_s \cdots D_{bc}$-Si structure.

We have also measured the vibrational line widths of the H stretching modes of the partially deuterated D_{ab}-$C_s \cdots H_{bc}$-Si and H_{ab}-$C_s \cdots D_{bc}$-Si structures. Table I shows that the line width of the H_{bc}-Si mode of the D_{ab}-$C_s \cdots H_{bc}$-Si structure is changed by only a small factor compared to the fully hydrogenated structure. However, the spectra in Fig. 1 and the line widths listed in Table I show that the width of the H_{ab}-C_s mode of the H_{ab}-$C_s \cdots D_{bc}$-Si center is changed dramatically, by a factor near 16, even though the mode frequency shifts only slightly.

Why do the C-H stretch modes of the H_{ab}-$C_s \cdots H_{bc}$-Si and H_{ab}-$C_s \cdots D_{bc}$-Si have such dramatically different line widths and vibrational lifetimes? The effect of isotopic substitutions on the lifetime of a vibrational mode can provide clues to the mechanism for vibrational relaxation. We turn to theory for an explanation of this surprisingly large isotope effect.

III. CALCULATIONS OF THE VIBRATIONAL LIFETIMES AND DECAY CHANNELS

A. Methodology

The approach used in the calculation of vibrational lifetimes and decay channels has been discussed in detail.[20] The key points are as follows. The host crystal is described by Si_{64} periodic supercells and the k-point sampling is restricted to the Γ point. This relatively small size and k-point sampling has been selected because many nonequilibrium MD runs are required in order to produce the needed averaging over initial mode phases and energies. This approach has been shown to produce accurate short as well as long lifetimes at various temperatures for almost 20 defects.[20–22]

The electronic structure calculations are based on the SIESTA[23,24] method. Norm-conserving pseudopotentials in the Kleinman-Bylander form[25] are used to remove the core regions from the calculations. The valence regions are treated self-consistently within local density-functional theory with

the exchange-correlation potential of Ceperley-Alder[26] as parameterized by Perdew-Zunger.[27] The basis sets for the valence states (double zeta for H or D, with polarization functions for Si) are linear combinations of numerical atomic orbitals of the Sankey type.[28] The charge density is projected on a real-space grid with equivalent cutoffs of 250 Ry to calculate the exchange-correlation and Hartree potentials. The dynamical matrices are calculated using the frozen-phonon method.

The eigenvalues of the dynamical matrix are the normal-mode frequencies ω_s. The corresponding orthonormal eigenvectors $e^s_{\alpha i}$ (where $i = x,y,z$) give the relative displacements of the nucleus α for each mode s. A quantitative measure of the localization of a given mode is on one atom or group of atoms is given by a plot of $L^2_{\{\alpha\}} = (e^s_{\alpha x})^2 + (e^s_{\alpha y})^2 + (e^s_{\alpha z})^2$ vs ω. The index $\{\alpha\}$ may be a single atom (e.g., H) or a sum over a group of atoms (e.g., the Si nearest neighbors to H).

The eigenvectors $e^s_{\alpha i}$ are used to transform the (harmonic) normal mode coordinates q_s into Cartesian nuclear displacements $u_{\alpha i} = \sum_s q_s\, e^s_{\alpha i}/\sqrt{m_\alpha}$. The simplest relationship, $q_s = A_s(T)\cos(\omega_s t + \varphi_s)$, assumes that the normal modes are harmonic. This is of course an approximation but it is needed to calculate the positions and velocities of the nuclei at the time $t = 0$ as well as the amplitudes of the various modes at subsequent times. The MD simulations themselves use forces calculated from first-principles total energies and therefore include all the anharmonic terms. Note that q_s introduces an initial random distribution of mode phases φ_s.

At $t = 0$, the supercell is prepared in thermal equilibrium at $T = 100$ K, and the excited LVM is given $3\hbar\omega/2$ potential energy using the appropriate eigenvector of the dynamical matrix. This background temperature is sufficiently high for the classical MD runs to accurately describe the phonon dynamics.[20,21] The initial potential energy of the excited mode corresponds to the zero-point energy plus one phonon, which guarantees that the (theoretical) classical and (experimental) quantum oscillators have the same initial amplitude. The added potential energy in this Si_{64} cell results in the net temperature to increase to ~120 K. Since the IR line widths are measured at low T, the calculated τ's are expected to be somewhat shorter than the low-T ones [measured $\tau(T)$ are in Refs. 17,18,29–31].

The amplitudes of all the normal modes in the supercell are obtained by assuming that the *average* kinetic energy of each mode is $k_B T/2$ which introduces a random distribution of energies that averages out to $k_B T$.[20] Thus, each MD run begins with a random distribution of mode phases and energies. Each calculation involves averaging over 20 to 27 different sets of initial conditions.

B. Vibrational lifetimes and receiving modes

We are interested here in the lifetime and decay channels of the H_{ab}-C_s stretch mode in H_{ab}-$C_s \cdots H_{bc}$-Si with all the possible D substitutions. The localized modes associated with this defect are the two H stretch modes, the corresponding two doubly degenerate H wag modes, as well as the doubly degenerate wag mode of C. Since the defects have trigonal symmetry, the wag modes are not possible receiving modes for the decay of the stretch modes because they are orthogonal and no momentum can be transferred.

TABLE II. Localized stretch and wag (doublets) vibrational modes of H_{ab}-$C_s \cdots H_{bc}$-Si with D substitutions and the associated localization (see text). The experimental values are in parentheses. Values marked with * are taken from Ref. 15.

Mode	Frequency (cm^{-1})	L^2_α
H_{ab}-C_s stretch	2567 (2688.3)	0.92
H_{ab}-C_s wag	1036	0.96
H_{bc}-Si stretch	2183 (2210.4)	0.96
H_{bc}-Si wag	556	0.35
C_s wag	685	0.77
H_{ab}-C_s stretch	2564 (2688.6)	0.93
H_{ab}-C_s wag	1036	0.96
D_{bc}-Si stretch	1568 (1606.5*)	0.94
D_{bc}-Si wag	332	0.48
C_s wag	685	0.77
D_{ab}-C_s stretch	1870	0.86
D_{ab}-C_s wag	757	0.75
H_{bc}-Si stretch	2190 (2214.7)	0.96
H_{bc}-Si wag	556	0.35
C_s wag	673	0.58
D_{ab}-C_s stretch	1876	0.86
D_{ab}-C_s wag	757	0.75
D_{bc}-Si stretch	1566 (1607.3*)	0.94
D_{bc}-Si wag	332	0.48
C_s wag	672	0.57

The calculated frequencies and localizations of all these modes are given in Table II for ^{12}C, ^{28}Si, and the various H/D isotope combinations. In three of the four isotope combinations, the H_{ab}-C_s (or D_{ab}-C_s) stretch mode is the highest-frequency mode. In these three cases, one of the receiving modes is the corresponding H_{bc}-Si (or D_{bc}-Si) stretch

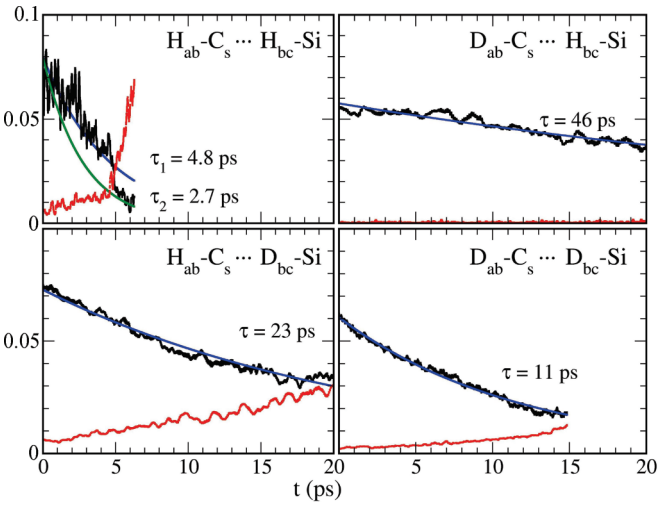

FIG. 2. (Color online) Energy (eV) of the H_{ab}-C_s (or D_{ab}-C_s) stretch mode (black) and of the H_{bc}-Si (or D_{bc}-Si) stretch mode (red) vs time (ps), calculated at $\sim T = 120$ K. In three of the four isotope combinations, the H_{bc}-Si (or D_{bc}-Si) stretch mode is a receiving mode. The missing energy is provided by one (or more) bulk phonon(s). In H_{ab}-$C_s \cdots H_{bc}$-Si, the decay does not fit to one exponential. The two fits shown provide lower and upper limits to the lifetime.

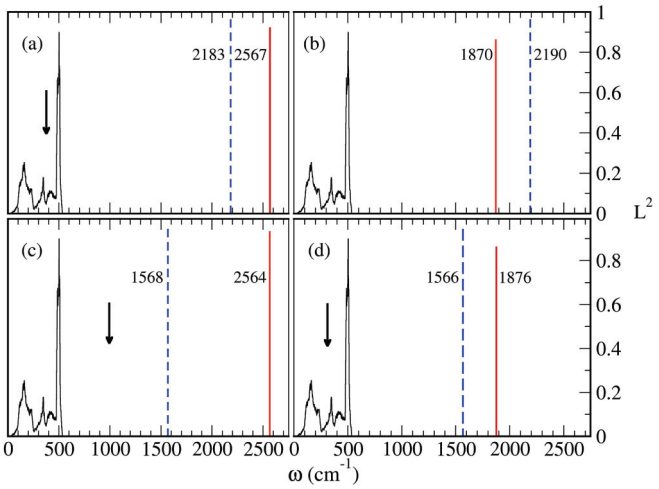

FIG. 3. (Color online) The two vertical lines show the localization L^2 (right scale) of the H_{ab}-C_s or D_{ab}-C_s (solid red line) and H_{bc}-Si or D_{bc}-Si (dashed blue line) modes. The calculated phonon density of states of Si is shown in black (arbitrary units). In three cases, the arrow points to the bulk phonon frequency $\Delta\omega$ required to complete the decay. (a) H_{ab}-$C_s \cdots H_{bc}$-Si. (b) D_{ab}-$C_s \cdots H_{bc}$-Si. (c) H_{ab}-$C_s \cdots D_{bc}$-Si. (d) D_{ab}-$C_s \cdots D_{bc}$-Si.

mode, and the missing energy is provided by one (or more) bulk phonon(s). However, in the case of D_{ab}-$C_s \cdots H_{bc}$-Si, the highest-frequency mode is H_{bc}-Si and the excited D_{ab}-C_s decays slowly directly into a combination of bulk phonons.

Figure 2 shows the calculated decays of the H_{ab}-C_s (or D_{ab}-C_s) mode and of the corresponding receiving H_{bc}-Si (or D_{bc}-Si) mode. Figure 3 shows the localization of the two stretch modes, the calculated phonon density of states of Si and, in three cases, the frequency of the bulk phonon required to complete the decay. The calculated lifetimes for the four isotope combinations are compared to the ones estimated from the IR line width in Table III.

IV. DISCUSSION

The excitation of defect-related LVMs leads to the trapping of a phonon by the defect. The trapped energy decays into combinations of lower frequency phonons after a length of time τ, the vibrational lifetime. The value of τ can depend critically on the existence, symmetry, and frequency of another LVM associated the defect. When such a second LVM exists, the lifetime of a high-frequency mode can be short and strongly affected by the isotopic composition of the defect.

The defect of interest here has two stretch modes, H_{ab}-C_s (or D_{ab}-C_s) with frequency ω_C and H_{bc}-Si (or D_{bc}-Si) with frequency ω_{Si}. In D_{ab}-$C_s \cdots H_{bc}$-Si, $\omega_C = 1870\ \text{cm}^{-1} < \omega_{Si} = 2190\ \text{cm}^{-1}$ and ω_C can only decay via multiple bulk phonons with a theoretical lifetime $\tau = 46$ ps. For the other three isotope combinations, $\omega_C > \omega_{Si}$ and the decay is of the type $\omega_C \rightarrow \omega_{Si} + \Delta\omega$.

For H_{ab}-$C_s \cdots H_{bc}$-Si, $\Delta\omega = 384\ \text{cm}^{-1}$ and numerous bulk phonons are available. This decay is a fast two-phonon process with a theoretical lifetime in the range $2.7 < \tau < 4.8$ ps and the IR line is broad. For H_{ab}-$C_s \cdots D_{bc}$-Si, $\Delta\omega = 996\ \text{cm}^{-1}$, far above the optical phonon of Si, and two bulk phonons are required. The decay becomes a much slower three-phonon process, the theoretical lifetime increases to $\tau = 23$ ps, and the IR line becomes very narrow. For D_{ab}-$C_s \cdots D_{bc}$-Si, $\Delta\omega = 310\ \text{cm}^{-1}$ and the predicted 11 ps lifetime is about average for a typical two-phonon decay.[19]

This is not an isolated situation. For example, another unexpected isotope effect has been reported in the case of interstitial oxygen (O_i) in Si.[22] The excited asymmetric stretch of O_i (ω_O) decays into the symmetric stretch of its two Si nearest neighbors (ω_{Si}) plus $\Delta\omega$. For the isotope combination ^{28}Si-^{16}O-^{28}Si, $\Delta\omega$ is $\sim$530 cm^{-1}, near or at the peak of the Si phonon density of states. Plenty of phonons are available and the decay is a two-phonon process. However, the isotope substitutions ^{29}Si-^{16}O-^{28}Si and ^{30}Si-^{16}O-^{28}Si cause ω_{Si} to shift to lower frequencies, and then $\Delta\omega$ increases just beyond the edge of the phonon density of states where few (or no) bulk phonons are available. As a result, τ increases from 11 ps (^{28}Si-^{16}O-^{28}Si, $\omega_O = 1136\ \text{cm}^{-1}$) to 27 ps (^{30}Si-^{16}O-^{28}Si, $\omega_O = 1129\ \text{cm}^{-1}$) as the two-phonon process becomes a three-phonon process.

The coupling of an isolated high-frequency LVM to a lower frequency phonon bath has been discussed by Nitzan and Egorov.[32,33] The theory works as long as none of the receiving modes is a defect-related LVM as well. A well-illustrated example[18,30] is the failure to fit the temperature dependence of the vibrational lifetimes of two similar H-related stretch modes in Si: a (measured) $\sim$300 ps lifetime fits nicely to a five-phonon decay while a much shorter $\sim$4 ps lifetime could only be fitted to a six-phonon decay. The presence of a second LVM in the latter case is the culprit.[20,21] In the present study, the extreme sensitivity of the vibrational lifetime to the isotopic makeup of the H_{ab}-$C_s \cdots H_{bc}$-Si defect betrays the identity of the receiving LVM that plays the critical role in the decay channel.

TABLE III. Vibrational lifetimes τ (in ps) of the H_{ab}-C_s (or D_{ab}-C_s) stretch mode calculated at $\sim T = 120$ K and extracted from the measured FWHM at 4.2 K.

Defect	Theory	Experiment
H_{ab}-$C_s \cdots H_{bc}$-Si	2.7–4.8	2.4
H_{ab}-$C_s \cdots D_{bc}$-Si	23	39
D_{ab}-$C_s \cdots H_{bc}$-Si	46	
D_{ab}-$C_s \cdots D_{bc}$-Si	11	

ACKNOWLEDGMENTS

This work at TTU is supported in part by Grant No. D-1126 from the R. A. Welch Foundation. Texas Tech's High Performance Computer Center provided generous amounts of CPU time. We are grateful to H. Zhang for making H stretching spectra he measured for Ref. 5 available for our study of vibrational line widths. The work at LU was supported by NSF Grant No. DMR 1160756 and by the NSF REU Program Grant No. PHY-0849416.

*stefan.estreicher@ttu.edu

[1] F. Duerinckx and J. Szlufcik, Sol. Energy Mater. Sol. Cells **72**, 231 (2002).

[2] F. Jiang, M. Stavola, A. Rohatgi, D. Kim, J. Holt, H. Atwater, and J. Kalejs, Appl. Phys. Lett. **83**, 931 (2003).

[3] S. Kleekajai, F. Jiang, M. Stavola, V. Yelundur, K. Nakayashiki, A. Rohatgi, G. Hahn, S. Seren, and J. Kalejs, J. Appl. Phys. **100**, 093517 (2006).

[4] I. A. Veloarisoa, M. Stavola, D. M. Kozuch, R. E. Peale, and G. D. Watkins, Appl. Phys. Lett. **59**, 2121 (1991).

[5] C. Peng, H. Zhang, M. Stavola, V. Yelundur, A. Rohatgi, L. Carnel, M. Seacrist, and J. Kalejs, J. Appl. Phys. **109**, 053517 (2011).

[6] G. Davies and R. C. Newman, in *Handbook on Semiconductors*, Vol. 3B, *Materials, Properties, and Preparation*, edited by S. Mahajan and T. S. Moss (North-Holland, Amsterdam, 1994), p. 1557.

[7] R. E. Pritchard, M. J. Ashwin, J. H. Tucker, and R. C. Newman, Phys. Rev. B **57**, R15048 (1998).

[8] A. W. R. Leitch, V. Alex, and J. Weber, Phys. Rev. Lett. **81**, 421 (1998).

[9] E. E. Chen, M. Stavola, W. Beall Fowler, and P. Walters, Phys. Rev. Lett. **88**, 105507 (2002).

[10] E. V. Lavrov, L. Hoffmann, B. Bech Nielsen, B. Hourahine, R. Jones, S. Öberg, and P. R. Briddon, Phys. Rev. B **62**, 12859 (2000).

[11] S. K. Estreicher, A. Docaj, M. B. Bebek, D. J. Backlund, and M. Stavola, Phys. Stat. Sol. A **209**, 1872 (2012).

[12] C. Peng, H. Zhang, M. Stavola, W. B. Fowler, B. Esham, S. K. Estreicher, A. Docaj, L. Carnel, and M. Seacrist, Phys. Rev. B **84**, 195205 (2011).

[13] P. Leary, R. Jones, and S. Öberg, Phys. Rev. B **57**, 3887 (1998).

[14] V. P. Markevich, L. I. Murin, J. Hermansson, M. Kleverman, J. L. Lindström, N. Fukata, and M. Suezawa, Physica B **302–303**, 220 (2001).

[15] B. Hourahine, R. Jones, S. Öberg, P. R. Briddon, V. P. Markevich, R. C. Newman, J. Hermansson, M. Kleverman, J. L. Lindström, L. I. Murin, N. Kukata, and M. Suezawa, Physica B **308–310**, 197 (2001); Defects and Diff. Forum **221–223**, 1 (2003).

[16] J. L. McAfee and S. K. Estreicher, Physica B **340–342**, 637 (2003).

[17] G. Lüpke, N. H. Tolk, and L. C. Feldman, J. Appl. Phys. **93**, 1 (2003).

[18] M. Budde, G. Lüpke, E. Chen, X. Zhang, N. H. Tolk, L. C. Feldman, E. Tarhan, A. K. Ramdas, and M. Stavola, Phys. Rev. Lett. **87**, 145501 (2001).

[19] B. Sun, G. A. Shi, S. V. S. Nageswara Rao, M. Stavola, N. H. Tolk, S. K. Dixit, L. C. Feldman, and G. Lüpke, Phys. Rev. Lett. **96**, 035501 (2006).

[20] D. West and S. K. Estreicher, Phys. Rev. B **75**, 075206 (2007).

[21] D. West and S. K. Estreicher, Phys. Rev. Lett. **96**, 115504 (2006).

[22] K. K. Kohli, G. Davies, N. Q. Vinh, D. West, S. K. Estreicher, T. Gregorkiewicz, I. Izeddin, and K. M. Itoh, Phys. Rev. Lett. **96**, 225503 (2006).

[23] D. Sánchez-Portal, P. Ordejón, E. Artacho, and J. M. Soler, Int. J. Quant. Chem. **65**, 453 (1997).

[24] E. Artacho, D. Sánchez-Portal, P. Ordejón, A. García, and J. M. Soler, Phys. Status Solidi B **215**, 809 (1999).

[25] L. Kleinman and D. M. Bylander, Phys. Rev. Lett. **48**, 1425 (1982).

[26] D. M. Ceperley and B. J. Adler, Phys. Rev. Lett. **45**, 566 (1980).

[27] S. Perdew and A. Zunger, Phys. Rev. B **23**, 5048 (1981).

[28] O. F. Sankey and D. J. Niklewski, Phys. Rev. B **40**, 3979 (1989); O. F. Sankey, D. J. Niklewski, D. A. Drabold, and J. D. Dow, *ibid.* **41**, 12750 (1990).

[29] M. Budde, G. Lüpke, C. Parks Cheney, N. H. Tolk, and L. C. Feldman, Phys. Rev. Lett. **85**, 1452 (2000).

[30] G. Lüpke, X. Zhang, B. Sun, A. Fraser, N. H. Tolk, and L. C. Feldman, Phys. Rev. Lett. **88**, 135501 (2002).

[31] M. Budde, C. Parks Cheney, G. Lüpke, N. H. Tolk, and L. C. Feldman, Phys. Rev. B **63**, 195203 (2001).

[32] A. Nitzan and J. Jortner, Mol. Phys. **25**, 713 (1973); A. Nitzan, S. Mukamel, and J. Jortner, J. Chem. Phys. **60**, 3929 (1974).

[33] S. A. Egorov and J. L. Skinner, J. Chem. Phys. **103**, 1533 (1995).